Empty-electronic-state evolution for Sc and electron dynamics at the 3p-3d giant dipole resonance

Yongjun Hu, T. J. Wagener, Y. Gao, and J. H. Weaver
Department of Materials Science and Chemical Engineering, University of Minnesota, Minneapolis, Minnesota 55455
(Received 6 December 1988)

Inverse photoemission has been used to study the developing electronic states of an early transition metal, Sc, during thin-film growth and to investigate the effects of these states on the 3p-3d giant dipole resonance. Energy- and coverage-dependent intensity variations of the empty Sc states show that the 3d maximum moves 1.1 eV toward the Fermi level as the thickness of the Sc film increases from 1 to 300 Å as measured with an incident electron energy of 41.25 eV, an effect attributed to metallic band formation via hybridization of atomic 4s and 3d states. Incident-energy-dependent intensity variations for these empty Sc features show resonant photon emission for incident electron energies above the 3p threshold, with maxima at 43 and 44 eV for 300- and 5-Å-thick films, respectively. Considerations of hybridization-induced energy shifts of the empty Sc 3d states demonstrate that the radiative energy changes very little with Sc coverages. These studies indicate coupling of decay channels involving the inverse photoemission continuum and the recombination of the atomic 3p-3d giant dipole transition, the energy of the latter being determined by atomic 3p-3d excitation processes.

INTRODUCTION

Electron emission intensities in electron-excited Auger spectra and photoemission cross sections for the 3d valence states are dominated by the 3p-3d giant dipole resonance in the 3p threshold region of the early 3d transition metals and Ca.[1-5] This is reflected by the 10–15-eV delay in the 3p-3d resonance.[1-6] This resonance is associated with interference between the $3p^6 3d^N \rightarrow 3p^5 3d^{N+1}$ and $3p^6 3d^N \rightarrow 3p^6 3d^{N-1} + \varepsilon l$ transitions, coupled via the super-Coster-Kronig transition $3p^5 3d^{N+1} \rightarrow 3p^6 3d^{N-1} + \varepsilon l$, namely the dependence of the atomic multiplet terms associated with the $3p^5 3d^{N+1}$ configurations.[7,8]

Recently, Barth *et al.*[1] compared the 3d photoemission cross section in the 3p threshold region for a 4-Å-thick Cr film to that for metallic Cr. Differences in 3d cross sections in the 3p-3d region were attributed to collective solid-state excitations that interacted with the 3p-3d resonance excitation.[1] Their results reflected the dynamics of excitation, ionization, and decay as solid-state effects became important. Earlier photoemission results had also shown solid-state modulation of subshell cross sections far above threshold.[9,10] The analogous resonant process may occur in inverse photoemission as long as core-level excitation or ionization occurs. In some cases, the interaction of the incident electrons with the atom can give rise to additional discrete states above the Fermi level,[11-13] and this complicates the electron dynamics of inverse photoemission relative to photoemission.

To further investigate the influence of atomic, solid-state, and dynamic effects, we have used inverse photoemission to examine the empty states of Sc and the dependence of the 3p-3d resonance on electron configuration. To do so, we have grown ultrathin and relatively thick films of Sc on graphite, thereby relating changes with the evolving-empty-electronic states. For thick films in normal incidence, the Sc 3d empty-state intensity shows a strong interferencelike resonance ~14–15 eV above the 3p core-level threshold, following a minimum 5–6 eV above threshold. For a 5-Å-thick Sc film, there is a sharper, more pronounced resonance shifted ~1 eV to higher incident electron energy. When account is taken of the hybridization shift in the evolving-3d-empty states, we conclude that the energy for the resonance is relatively insensitive to the atomic environment, although the interference minimum for a 5-Å-thick film becomes weaker. Our results for 10–20-Å-thick films show strongly enhanced Sc 3d intensities, and we attribute the effect to either localized empty final states or boundary scattering in Sc clusters. Similar enhancement has been found in photoabsorption and photoyield studies of small particles.[14-16]

EXPERIMENT

The experiments were performed in a spectrometer optimized for both ultraviolet and x-ray photon emission studies,[17] although the present studies emphasized the ultraviolet photon energy range in the vicinity of the Sc 3p threshold (10–44 eV). A highly collimated monoenergetic electron beam was directed onto the sample surface from an electron gun with a $1 \times 5 mm^2$ planar BaO cathode and Pierce-type geometry. Within the sample, electrons that radiatively decay from high-lying states at energy E_i to lower-lying states at E_f, produced photons of energy $h\nu = E_i - E_f$. These emitted photons were dispersed by a near-normal-incidence grating monochromator and were detected with a position-sensitive detec-

tor. The combined energy resolution (electrons and photons) was 0.3–0.6 eV, depending on photon energy. The angle between the incident electron beam and outgoing photon beam was fixed at 60°. Spectrometer calibration and normalization procedures have been described elsewhere.[17] The operating pressure of the experimental system was $\sim 8\times 10^{-11}$ Torr.

Scandium was evaporated from resistively heated sources at pressures $\sim 2\times 10^{-10}$ Torr. The substrates were highly oriented pyrolytic graphite (HOPG) that had been prepared by cleaving *in situ* to produce fresh basal-plane surfaces. The amount of deposited material was determined with a quartz crystal oscillator adjacent to the sample. Auger electron spectroscopy studies served to independently check the sample and substrate cleanliness. The deposition of 200–300 Å of Sc gave metallic films with electronic properties that had converged to those of the metal. For these thick films, the HOPG substrate emission was no longer discernible.[18]

RESULTS AND DISCUSSION

Energy states and thin-film morphology

In order to examine the empty electronic states for Sc thin films grown on graphite, we measured photon-distribution curves (PDC's) as a function of deposition for coverages $0.25 \leq \Theta \leq 200$ Å. Representative PDC's taken at $E_i = 24.25$ eV are shown in Fig. 1, normalized to electron dose. The amount of Sc deposited is given alongside each PDC; 1 Å of Sc corresponds to $\sim 4\times 10^{14}$ at/cm^2. The spectrum for the clean surface is dominated by graphite $\sigma(\Gamma_5^+, \Gamma_6^-)$ bulk state emission 9.5 eV above the Fermi level E_F, and there is emission involving a graphite surface state at 3.5 eV.[18] For very low coverages of 0.25–1.5 Å, the photon emission intensity involving states near E_F is small and flat. For Sc coverages above ~ 6 Å, however, the empty-state emission just above E_F grows and Sc 3*d* state emission clearly develops.

To characterize the growth morphology of these Sc films on HOPG, we determined the rate at which the substrate $\sigma(\Gamma_5^+, \Gamma_6^-)$ bulk feature was attenuated. The results based on PDC's taken at $E_i = 24.25$ eV are shown in Fig. 2 where the emission at a coverage Θ has been normalized to that for the clean surface. For coverages below ~ 3 Å, the substrate feature is linearly attenuated (on a semilog plot) but it is much more slowly attenuated at higher coverage. This is typical for Stranski-Krastanov[19] growth, i.e., cluster growth over a surface layer. Even at 25-Å deposition, the $\sigma(\Gamma_5^+, \Gamma_6^-)$ graphite feature persists at the e^{-3} level.

A rough idea of the Sc cluster size on HOPG can be obtained by assuming hemispherical growth on a uniform monolayer (ML) of Sc. By using the average nucleation site concentration n_c as a fitting parameter,[18] this model for normal incidence of electrons predicts substrate attenuation of the form

$$\ln\left[\frac{I(\Theta)}{I(0)}\right] = \begin{cases} \ln\left\{1-n_c\pi R^2\left\{1+\frac{2}{R^2}\left[(R\lambda_e+\lambda_e^2)\exp\left[\frac{-R}{\lambda_e}\right]-\lambda_e^2\right]\right\}\right\} - \frac{d}{\lambda_e} & \text{for 1 ML} \leq \Theta \leq \Theta_c \\ -\frac{\Theta}{\lambda_e} \text{ for } \Theta \leq 1 \text{ ML}, \end{cases}$$

where λ_e is an effective mean free path, R (in Å) $=[(3n_c/2\pi)(\Theta - d)]$, d is the nominal monolayer thickness of 2.7 Å, and Θ_c is the coverage at which clusters coalesce. The electron mean free path is estimated to be ~ 2.7 Å. Comparison of fitting results (open circles) and experiment (solid circles) in Fig. 2 supports this simple morphology model in an average sense. In the early cluster formation stage for Sc depositions ~ 3–13 Å, the fitting density was $n_c = 4\times 10^{12}$ cm^{-2}.

In Fig. 3 we present PDC's as a function of Sc deposition for $E_i = 41.25$ eV to show the coverage-dependent variation of the empty electronic structures at resonance (resonance will be described in detail in subsequent paragraphs). The graphite substrate contribution has been subtracted from all of the spectra. The movement of the 3*d* peak position is summarized at the top of Fig. 3. From them, we can conclude that the *d* bands have converged to their final metallic configuration by $\Theta \sim 20$ Å. They exhibit a total shift of 0.7 eV for thick films relative to the 5-Å-ultrathin films case. The evolution of the empty electronic states of Sc, with the appearance of emission at E_F and a shift in the *d* bands, can be interpreted in terms of size-dependent hybridization between the unoccupied Sc 3*d* levels and the occupied 4*s* states. Moruzzi and Marcus[20] have predicted that the number of 3*d* electrons that hybridize with the 4*s* bands in metallic Sc will be 1.6.

In previous inverse photoemission studies,[18] we found that clusters with an average radius of ~ 17.6 Å for Au and ~ 13.6 Å for Pd, containing ~ 670 and ~ 370 atoms, showed characteristics indicative of bulk metal behavior. For Sc, the growth morphology appears to be more complicated and a clear correlation of deposition with cluster size is not possible. One common result for Sc and Pd is that the density of *d* states at the Fermi level is very small at low coverage. For atomic Pd, the 4*d* states are fully occupied and clustering results in their hybridization with the empty *s* and *p* states. At ~ 2 Å of Pd, the empty 4*d* feature appears just above the Fermi level. In contrast, the Sc atomic configuration is $4s^2 3d^1$ and hybridi-

zation between the 4*s* states and the unoccupied 3*d* states increases the 3*d*-4*s* overlap so that the Sc 3*d* feature shifts toward E_F. These results for early and late transition metals indicate that hybridization induces opposite movements of the *d* states.

Energy- and coverage-dependent intensity variations of Sc 3*d* empty states

In Fig. 4 we show representative normal incidence PDC's for a fully metallic 300-Å Sc film for incident electron energies ranging from 22.25 to 44.25 eV measured relative to the sample Fermi level. The spectra have been normalized to electron dose and spectrometer throughput so that intensity changes are quantitative. Since the abscissa corresponds to constant photon energy, E_F moves to the left with increasing E_i (arrows). The main feature ~3 eV above E_F corresponds to the maximum of the 4.5-eV-wide Sc 3*d* empty states and is identified by tick marks. As can be seen from the relative intensity of the main *d* feature, there is a dramatic minimum when E_i crosses the Sc 3*p* threshold (minimum at $E_i \sim 34$ eV), but the 3*d* intensity quickly recovers and exhibits a maximum at $E_i \sim 43$ eV. The broad, constant-photon-energy features from ~20 to ~28 eV are a result of fluorescent decay involving incident-electron-induced 3*p* core holes. These fluorescence features exhibit a pronounced edge at a photon energy of 28.3 eV (identified as the $M_{2,3}$ edge[21] in Fig. 4) and overlap with a plasmon-related photon emission feature at $h\nu \sim 22$ eV.[22]

To be quantitative in this assessment of the 3*d* cross section, we plot in Fig. 5 the intensity of the 3-eV peak as a function of incident electron energy. The results at the top are for a 300-Å metallic film while those at the bottom are for a 5-Å film. For the latter, the Sc 3*d* intensity was obtained by subtracting the contribution of the graphite substrate at each energy. The 5-Å film can be approximated as clusters beginning to grow on a Sc monolayer such that more than 85% of the Sc atoms are surface atoms and long-range, three-dimensional order has not yet developed. The results of Fig. 5 show intriguing cross-section differences for atomiclike and bulklike Sc films. In particular, the cross section for the thick film exhibits a strong maximum at $E_i = 43$ eV, compared to 44 eV for the 5-Å film, and the resonance enhancement is substantially broader for the thick film. For the thick

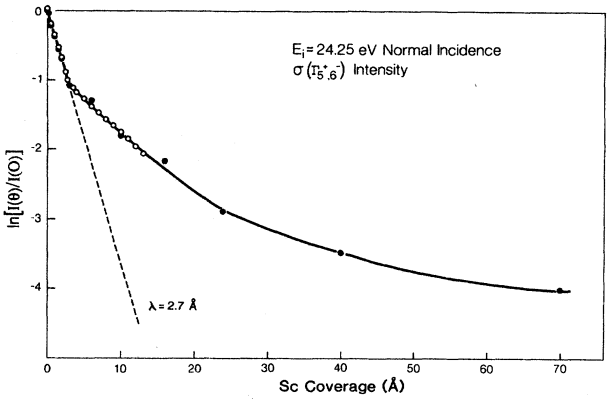

FIG. 2. Attenuation curves showing the rate at which the total integrated intensity of the empty $\sigma(\Gamma_5^+,\Gamma_6^-)$ bulk state of HOPG decreases as a function of Sc deposition. The straight line represents laminar growth with $\lambda_e \sim 2.7$ Å. The deviation from this behavior after ~1 ML deposition indicates cluster growth. The solid circles are experimental results while the open circles are calculated based on the Stranski-Krastanov growth mode.

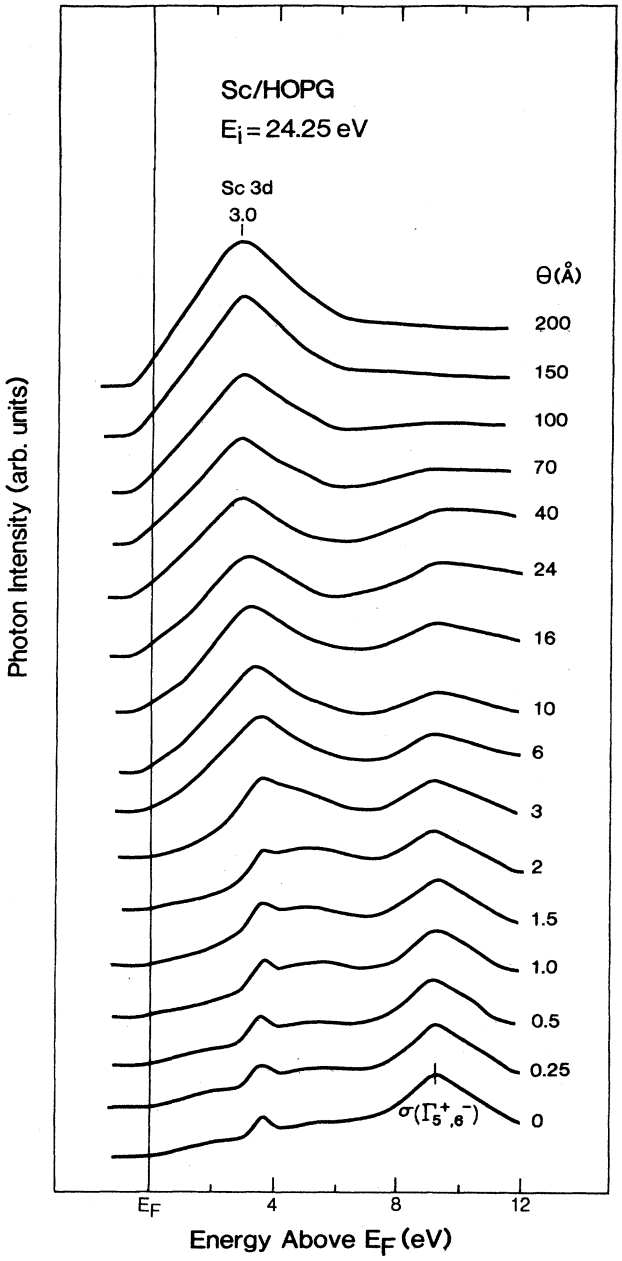

FIG. 1. Normal-incidence photon-distribution curves (PDC's) for Sc depositions on HOPG taken at $E_i = 24.25$ eV. The amount of material deposited is given alongside each PDC.

film there is also a distinct minimum 5–6 eV above the $3p$ threshold but that minimum is much less pronounced for the 5-Å case.

Finally, in Fig. 6 we summarize the intensity variations for the Sc $3d$ feature as a function of coverage for incident electron energies of 24.25, 36.25, and 41.25 eV corresponding to excitation energies below the $3p$ threshold, above threshold, and on resonance. Each has a broad maximum at low coverage. The $3d$ intensities for $E_i = 36.25$ and 41.25 eV decrease slowly to a value at very high coverage that is approximately half the maximum value. The $3d$ intensity variation for $E_i = 24.25$ eV is more complicated because of a minimum near 30 Å and a gradual increase thereafter. This increase is related to the growth of an overlapping, constant-photon-energy plasmon feature near 22 eV and the growth of this plasmon feature as the film thickens.[22] Such coverage-dependent variations for empty d states have not been previously observed. In the following we consider their origin.

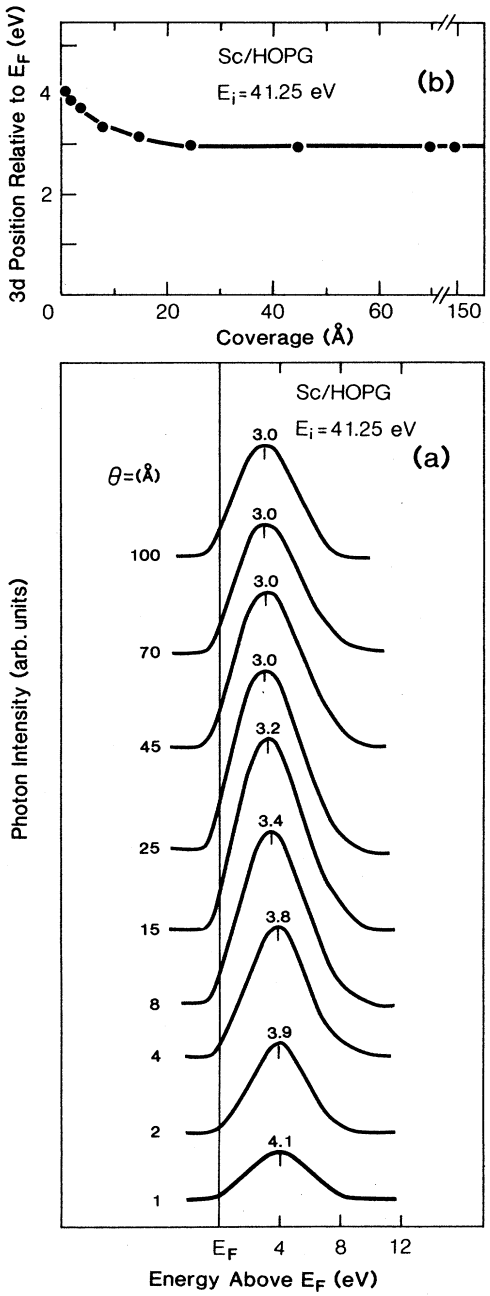

FIG. 3. (a) PDC's as a function of Sc deposition for $E_i = 41.25$ eV showing coverage-dependent variations in the Sc $3d$ states at resonance. (b) Summary of the energy of the Sc $3d$ feature as a function of coverage showing stabilization to a final position by ~20 Å.

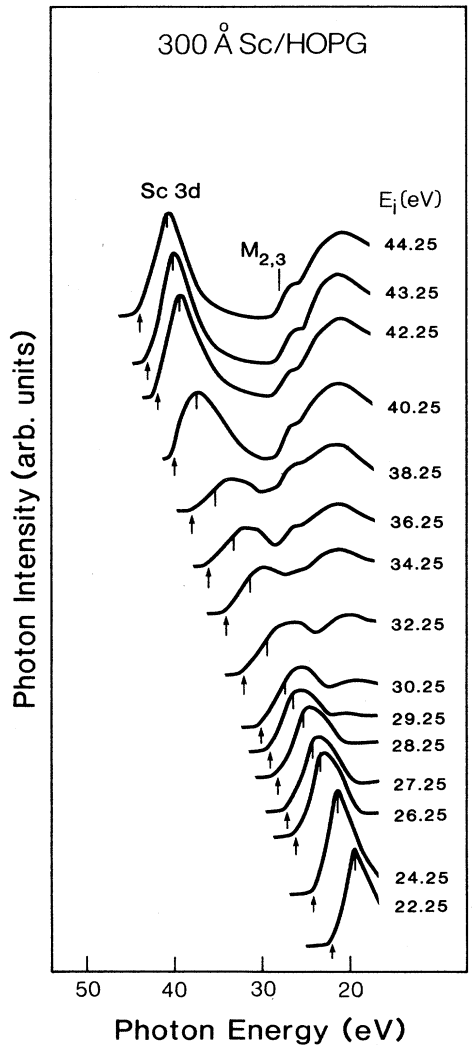

FIG. 4. PDC's for a 300-Å Sc film in normal incidence as a function of incident electron energy showing strong variation in the Sc $3d$ features. The Fermi level is indicated by arrows and the Sc $3d$ maximum is identified with tick marks. The constant photon energy peak near 26 eV is due to fluorescent decay of the $3p$ core hole. It overlaps a plasmon-related photon emission feature at ~22 eV.

The photon emission intensity in inverse photoemission is mainly determined by the capture cross section of the electrons in the low-lying states, here the evolving Sc $3d$ band. We propose, therefore, that the results of Fig. 6 directly reflect the details of these initial and final states and thus their matrix elements. Recently, Wendin[12] examined the x-ray emission in the $3d$ threshold region of La and showed that the decay to empty $4f$ final states was proportional to the cross section for direct bremsstrahlung radiative capture, $\sigma_{nl}(\omega;E_i)$, the line-shape function (spectra function) $A_{nl}(E_i;\omega)$ for the hybridization of the $4f$ level, and the x-ray fluorescence emission term $R(\omega;E_i)$ at fixed photon energy $\hbar\omega$ due to decay of the electron-induced core hole. The last term is associated with the enhancement of the radiative process. In a first approximation, the $R(\omega;E_i)$ term can be regarded as the enhancement contribution from the coupling effect implicit in $3p$ excitation, as mentioned above and discussed in the next section. Each of these should exhibit changes associated with the formation of the solid. Note, however, that recent experimental results suggest that contributions from features associated with plasmon-related photon emission or the surface dielectric response should also be taken into account in this term.[18,22,23]

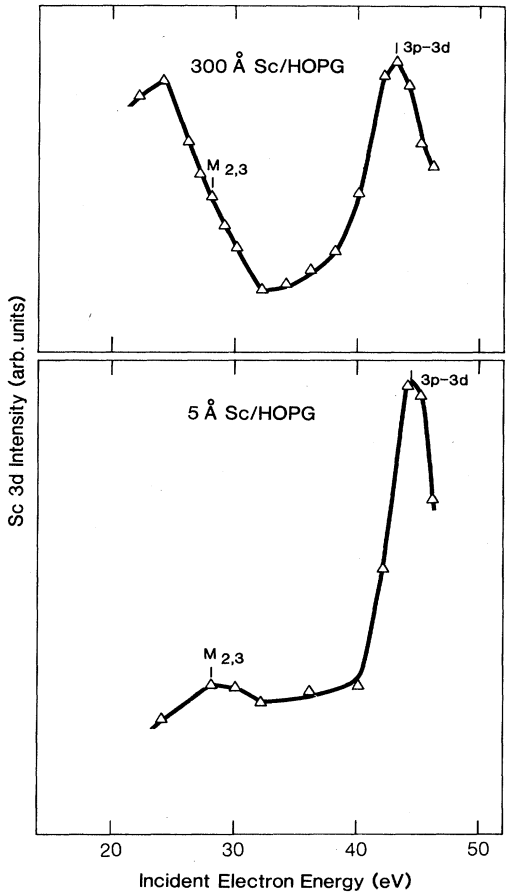

FIG. 5. The intensity variations of the Sc $3d$ empty state as a function of incident electron energy for a 300-Å film (top) and 5-Å film taken in normal incidence. The intensity curves exhibit strong Sc $3d$ enhancement at $E_i \sim 43$ eV for the thick film and ~ 44 eV for the thin film. A significant minimum of the Sc $3d$ intensity at $E_i \sim 5$–6 eV above the $3p$ threshold can be seen for a 300-Å metallic film while it is not so obvious for a 5-Å-thin film.

The maximum of the $3d$ emission in inverse photoemission occurs before the $3d$ state position is stabilized at $\Theta = 25$ Å. It can be speculated that the intensity variation is associated with the s-d hybridization as the clusters evolve into the extended solid. The intensity increases with deposition at low coverage ($\Theta < 20$ Å). As the cluster size or film thickness increases, s-d hybridization becomes significant and there is delocalization of some of the $3d$ states. This results in the reduction of $3d$ emission intensity. The data therefore provide a direct measurement of s-d hybridization. Such significant reduction for the $3d$ intensity probably reflects the changing $3d$ occupancy from 1 to ~ 1.6 from atom to solid, according to recent theoretical calculations.[20]

Mechanisms involving boundary scattering may also contribute to the size dependence cross sections observed in Fig. 6. In that case, electron scattering and momentum transfer will occur at the surface of the clusters and the extent should depend on the detailed morphology of the clusters. From Fig. 6, there appears to be a maximum in the photon emission when the clusters are small. This is consistent with results from studies where photoabsorption and photoyield enhancement was observed for small metal particles.[14–16]

Resonant inverse photoemission

In the $3d$ transition metals, resonant photoemission is associated with a $3p \rightarrow 3d$ giant dipole resonant excitation channel that can transfer energy to excite the $3d$ valence-band electrons ($3d \rightarrow \varepsilon l$) and enhance $3d$ valence-band emission at photon energies 10–15 eV above the $3p$ threshold.[1,3,4] The observed inverse-photoemission enhancement of the Sc empty-$3d$-state emission indicates that the incident electron can excite $3p$ electrons into $3p$-$3d$ resonant final states ~ 15 eV above E_F so that subsequent $3p$-$3d$ decay (a direct recombination process) leads to photon emission.[22] This couples with inverse-photoemission channels arising from the decay of incident electrons ~ 43 eV above E_F.

The results of Fig. 5 show that E_i for resonant excitation shifts 1 eV to lower energy for a 300-Å film relative to a 5-Å Sc film. This shift can be associated with the internal dynamics of the atomic $3p$-$3d$ giant dipole resonance. As we know, the energy of the resonance is determined primarily by atomic effects, namely the atomic response of the $3p$ core electron and the localization of the $3d$ states. As can be seen in Fig. 3, the Sc empty-$3d$-state features move 0.7 eV as the Sc film evolves from 5 to 300 Å. In order to maintain the radiative energy from E_i to final $3d$ states to couple with the $3p$-$3d$ process, E_i for resonance must decrease. The 0.3-eV difference in resonant photon energy can be considered as the difference between $3d$ states and the $3p$ core-level electrons because of band formation and charge redistribution.

The influence of hybridization is evident from the $3d$

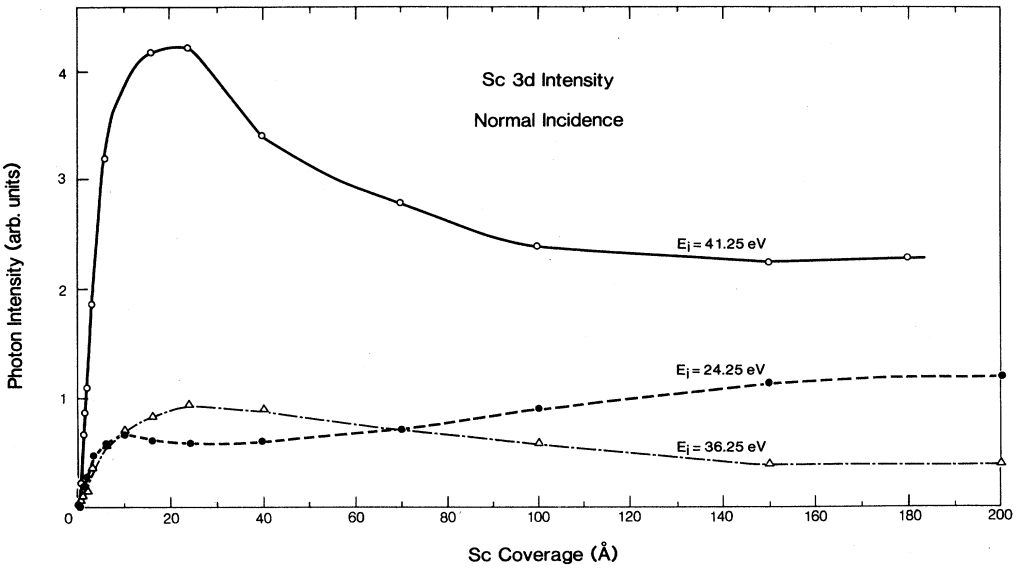

FIG. 6. Coverage-dependent Sc 3*d* intensity variations at fixed incident electron energies of $E_i = 24.25$, 36.25, and 41.25 eV. Enhancement in the low-coverage region can be seen in all cases, as discussed in the text. At very high coverage, the 3*d* intensities for $E_i = 36.25$ and 41.25 eV decrease and finally stabilize at a value about half of the maximum value. For $E_i = 24.25$ eV, overlap with the plasmon-related photon-emission feature produces the increase at high coverage.

intensity curves of Fig. 5. The maximum, which reflects the 3*p*-3*d* process coupling with the inverse photoemission continuum, is sharp for the 5-Å film and it broadens on the low-energy side for the 300-Å film. The broadening is interesting because it may be associated with dynamic effects with a $3p^5 3d^3$ intermediate state involving the incident electrons, i.e., electron impact resonance.[12] We suggest that broadening arises from the $3p^5 3d^3$ intermediate state, where a complex state consisting of three *d* electrons in the hole field will reduce the energy for radiative decay of the 3*p* hole.[12,13] Comparison of our inverse photoemission enhancement to that for the occupied 3*d* states of Sc (Ref. 1) shows a broader tail at lower photon energies for inverse measurements. A number of possible channels for electron impact resonance have been discussed in Ref. 12. The intensity reduction of the resonance feature for the 300-Å film in Fig. 5 can be understood in terms of the smaller 4*s* cross section and the delocalization of 3*d* empty states related to 4*s*-3*d* hybridization. Hence, the resonance amplitude strongly depends on the 3*d* occupancy. Suppression of the 3*d* resonance feature in photoemission has been found when comparing gas phase and solid-state Cr as the sharp Fano-type atomic resonance is broadened to higher energy for the solid.[1]

Another solid-state influence can be seen based in Fig. 5 since the minimum in the 3*d* intensities is more pronounced for the 300-Å film than for the 5-Å film. Analogous results have been reported from photoemission studies of gas phase and metallic Cr.[1] For Cr, Davis and Feldkamp[24] have incorporated the coherent continuous empty states in calculations of photoemission matrix elements. The calculation shows a pronounced interference dip for the Cr 3*d* cross sections at threshold. The inverse photoemission results show the existence of similar band effects near threshold.

CONCLUSIONS

We have examined the empty electronic state evolution for the early transition metal Sc. Inverse-photoemission results show coverage-dependent hybridization between the almost empty 3*d* and filled 4*s* states. As a result, the 3*d* bands move toward the Fermi level with increasing Sc deposition, with saturation by ~20 Å. The inverse-photoemission results show very strong coverage- and energy-dependent intensity variations of the Sc empty 3*d* states. The energy-dependent 3*d* intensity variations show a delayed onset with a maximum ~15 eV above threshold for a 300-Å metallic film and ~16 eV for a 5-Å film. However, the radiative energy for the cross-section maximum remains at ~40 eV when account is taken of shifts in the 3*d* feature. This indicates that the resonant process near the 3*p* threshold is dominated by coupling between the inverse-photoemission continuum and the recombination of the atomic 3*p*-3*d* giant dipole resonance transition. The energy of the latter depends only on the atomic 3*p*-3*d* excitation process. Hybridization or solid-state effects suppress the resonant enhancement and are responsible for the variation in shape for the resonance feature. It suggests that the resonance amplitude can be adjusted by hybridization or occupancy of the 3*d* states.

ACKNOWLEDGMENTS

This work was supported by the National Science Foundation under Grant No. DMR-86-10837.

[1]J. Barth, F. Gerken, and C. Kunz, Phys. Rev. B **31**, 2022 (1985).
[2]G. Zajac, S. D. Bader, A. J. Arko, and J. Zak, Phys. Rev. B **29**, 5491 (1984).
[3]J. Barth, F. Gerken, K. L. I. Kobayashi, J. H. Weaver, and B. Sonntag, J. Phys. C **13**, 1369 (1980).
[4]E. Bertel, R. Stockbauer, and T. E. Madey, Phys. Rev. B **27**, 1939 (1983).
[5]J. Barth, I. Chorkendorlf, F. Gerken, C. Kunz, R. Nyholm, J. Schmidt-May, and G. Wendin, Phys. Rev. B **30**, 6251 (1984).
[6]G. Wendin, in *New Trends in Atomic Physics,* edited by R. Stora and G. Grynberg (North-Holland, New York, 1983).
[7]R. E. Dietz, E. G. McRae, Y. Yafet, and C. W. Caldwell, Phys. Rev. Lett. **33**, 1372 (1974).
[8]L. C. Davis and L. A. Feldkamp, Solid State Commun. **19**, 413 (1976).
[9]S. Y. Tong and N. Stoner, J. Phys. C **11**, 3511 (1978).
[10]H. Peterson and C. Kunz, Phys. Rev. Lett. **35**, 863 (1975).
[11]G. Wendin and K. Nuroh, Phys. Rev. Lett. **39**, 48 (1977); K. Nuroh and G. Wendin, Phys. Rev. B **24**, 5533 (1981); J. Kanski and G. Wendin, Phys. Rev. B **24**, 4977 (1981).
[12]G. Wendin, in *Giant Resonances in Atoms, Molecules, and Solids,* edited by J. P. Connerade, J. M. Esteva, and R. C. Karnatak (Plenum, New York, 1987), pp. 171–211.
[13]P. Motais, E. Belin, and C. Bonnelle, Phys. Rev. B **30**, 4399 (1984).
[14]A. Schmidt-Ott, P. Schurterberger, and H. C. Siegmann, Phys. Rev. Lett. **45**, 1284 (1980); U. Kreibig, J. Phys. F **4**, 999 (1974).
[15]A. Kawabata and R. Kubo, J. Phys. Soc. Jpn. **21**, 1765 (1966); U. Kreibig and C. U. Fragsten, Z. Phys. **224**, 307 (1969); R. Ruppin and H. Yatom, Phys. Status Solidi B **74**, 674 (1976).
[16]D. R. Penn and R. W. Rendell, Phys. Rev. Lett. **47**, 1067 (1981); P. Apell and D. R. Penn, *ibid.* **50**, 1316 (1983).
[17]Y. Gao, M. Grioni, B. Smandek, J. H. Weaver, and T. Tyrie, J. Phys. E **21**, 488 (1988).
[18]Yongjun Hu, T. J. Wagener, Y. Gao, H. M. Meyer III, and J. H. Weaver, Phys. Rev. B **38**, 3037 (1988).
[19]R. Ludeke, J. Vac. Sci. Technol. B **2**, 400 (1984).
[20]V. L. Moruzzi and P. M. Marcus, Phys. Rev. B **38**, 1613 (1988).
[21]M. Cardona and L. Ley, *Photoemission in Solids* (Springer-Verlag, Berlin, 1978).
[22]Yongjun Hu, T. J. Wagener, Y. Gao, and J. H. Weaver, Phys. Rev. B **38**, 12 708 (1988).
[23]W. Drube and F. J. Himpsel, Phys. Rev. Lett. **60**, 140 (1988); W. Drube, F. J. Himpsel, and P. J. Feibelman, *ibid.* **60**, 2070 (1988).
[24]L. C. Davis and L. A. Feldkamp, Phys. Rev. B **15**, 2961 (1977); **23**, 6239 (1981).